Pergamon

Cement and Concrete Research, Vol. 27, No. 11, pp. 1719–1729, 1997

0008-8846/97 $17.00 + .00

PII S0008-8846(97)00156-7

THE FRACTURE CHARACTERISTICS OF CRUSHED LIMESTONE SAND CONCRETE

J.-K. Kim,* C.-S. Lee,* C.-K. Park,* and S.-H. Eo†

*Department of Civil Engineering, Korea Advanced Institute of Science and Technology, Taejon, Korea

†Department of Civil Engineering, Changwon National University, Changwon, Korea

(Refereed)

(Received January 3, 1997; in final form August 26, 1997)

ABSTRACT

The use of crushed sand as a fine aggregate has rapidly increased due to a shortage of river sand. Accordingly, research on crushed sand concrete is required. In this research, the fracture characteristics of crushed limestone sand concrete were experimentally investigated through a wedge splitting test, and the results were compared with those of crushed granite sand concrete and river sand concrete. The strength of crushed limestone sand concrete was also investigated. It was shown that the fracture energy of concrete was little influenced by the type of fine aggregate. In addition, the fracture energy of crushed sand concrete was slightly higher than that of river sand concrete. This seems to be due to very fine sand (VFS) included in crushed sand, which tends to improve the cohesion between cement paste and aggregate. Also, the fracture energy was not proportionally increased with an increase of concrete strength. The characteristic length of crushed limestone sand concrete was almost the same as that of river sand concrete or crushed granite sand concrete. The characteristic length greatly decreased as the strength of concrete increased. © *1997 Elsevier Science Ltd*

Introduction

Recently, the use of aggregate has rapidly increased because construction has expanded with rapid economic development. Due to the shortage of river sand, sea sand and crushed sand are being used in many construction sites. Crushed sand is different in shape, grading, and content of very fine sand (VFS) compared with river sand, and it is well known that the material properties of crushed sand concrete are also different from those of river sand concrete (1–3). However the fracture behavior of crushed sand concrete has been little researched. Accordingly, the difference in fracture behavior between crushed sand concrete and river sand concrete should be experimentally and theoretically investigated. Fracture energy (Gf) is a material property representing fracture toughness of concrete, and is defined as the amount of energy necessary to create the unit crack area. A three-point bend test on notched beams was proposed by RILEM to determine G_f (4). In addition, a wedge splitting

TABLE 1
Physical Properties of Crushed Limestone Sand

Specific gravity (in absolute dry condition)	2.68
Water absorption (%)	0.52
Content of VFS (%)	1.68
Unit weight (kg/m^3)	1748
Fineness modulus	2.96

test (WST) method proposed by Linsbauer was regarded as a promising test method for the determination of such fracture parameters as G_f and fracture toughness (5,6).

In this research, the fracture characteristics of crushed limestone sand concrete were investigated using the WST method, and the test results were compared with those of river sand concrete and crushed granite sand concrete. The strength of crushed limestone sand concrete was also investigated.

Material Properties of Crushed Limestone Sand

The crushed limestone sand used in this research was obtained from Donghae, Korea. The physical properties of crushed limestone sand are given in Table 1, and the grading curve is given in Figure 1. In Table 1, the content of VFS is the amount of material finer than a 75-μm (No. 200) sieve in fine aggregate.

A test for the soundness of crushed limestone sand was performed according to ASTM C 88. A sample of crushed limestone sand was alternately subjected to immersion in a saturated solution of sodium sulfate and drying in a oven. ASTM C 33 has regulated that fine aggregate

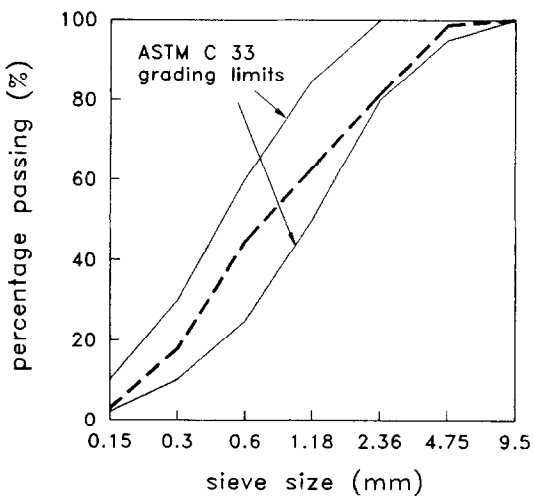

FIG. 1.
Grading curve of crushed limestone sand.

TABLE 2
Mix Proportions of Concrete

Mix Series	Mix No.	W/B (%)	Unit weight (kg/m^3)				Admixture (CX%)
			Cement	Water	Sand	Gravel	
I	W40	40	505	202	766	899	0.5
	W50	50	403	202	806	946	–
	W60	60	336	202	833	977	–
II	AGE	60	340	204	830	974	–
III	VFS	60	331	199	839	985	–

subjected to five cycles of a soundness test shall have a weighted average loss not greater than 10% when sodium sulfate is used. According to the test results, the weighted average loss of crushed limestone sand was 5.4%, thus satisfying the regulation of ASTM C 33.

The alkali-aggregate reaction was examined by the chemical method in ASTM C 289. From the test results, the reduction in alkalinity (R_c) was 201.5 mmol/liter, and the dissolved silica (S_c) was 15.4 mmol/liter. This test result of alkali-aggregate reaction for the crushed limestone sand used was considered as innocuous according to ASTM C 289.

Strength of Crushed Limestone Sand Concrete

Test Variables and Mix Proportions

In mix proportions, crushed limestone sand, mixed sand (50% crushed limestone sand plus 50% river sand), and river sand were used as fine aggregate. Mix series I was selected to test the strength with water-binder ratio, mix series II to test the strength with age, and mix series III to test the strength with the content of VFS. The VFS contents of adjusted crushed limestone sand are 0, 3, and 6% by weight of fine aggregate. Ordinary Portland cement (ASTM Type I) was used, and the crushed limestone gravel passing the 25-mm sieve was used as coarse aggregate. Detailed mix proportions are given in Table 2.

Test Results

The test results of strength characteristics of crushed limestone sand concrete are given in Figure 2 for the water-binder ratio, age, and content of VFS. According to test results, the strength of concrete using the mixed sand was superior at all water-binder ratios. In addition, the strength of crushed limestone sand concrete was slightly lower than that of river sand concrete.

The strength of crushed limestone sand concrete was almost the same as the strength of river sand concrete at 3 days, but at other ages it was a little lower than that of river sand concrete. The strength of concrete with 3% VFS was better than that of concrete with 0% VFS. However, the strength of concrete with 6% VFS was rather decreased as compared with that of concrete with 3% VFS. Accordingly, some limited contents of VFS tend to improve the strength of crushed limestone sand concrete.

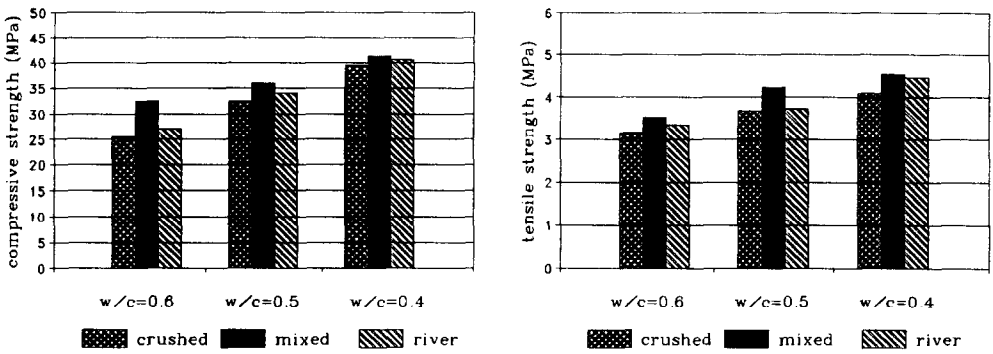

(a) Effect of water-binder ratio on concrete strength

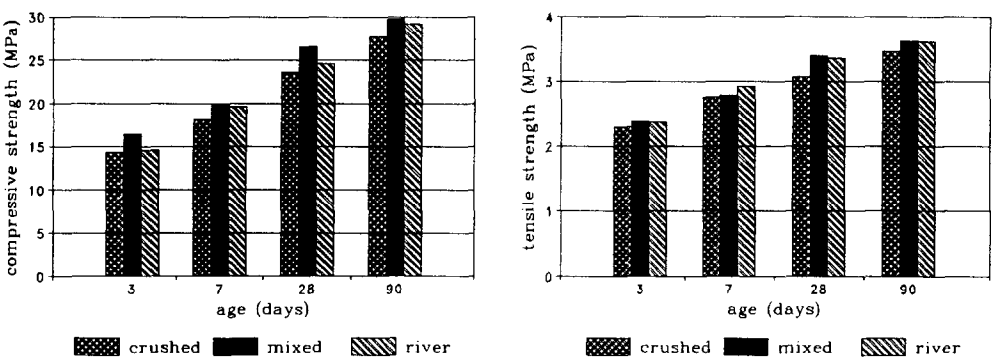

(b) Effect of age on concrete strength

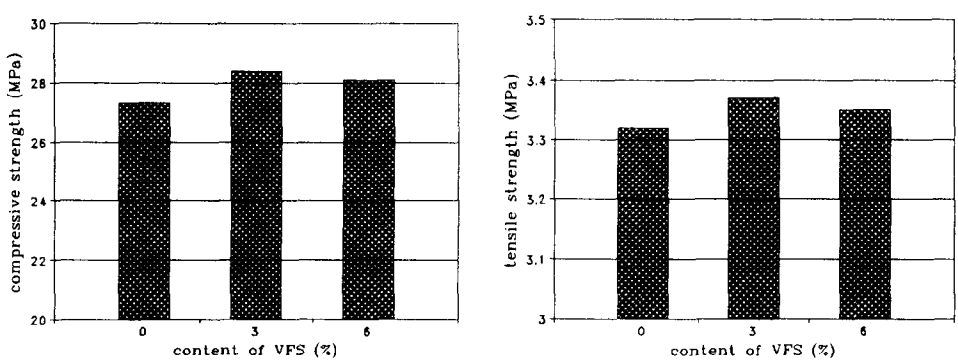

(c) Effect of content of VFS on concrete strength

FIG. 2.

Strength characteristics of crushed limestone sand concrete: (*a*) effect of water-binder ratio on concrete strength; (*b*) Effect of age on concrete strength; (*c*) effect of content of VFS on concrete strength.

TABLE 3
Physical Properties of Fine Aggregate

Fine aggregate	Specific gravity	Absorption (%)	F.M.
Crushed limestone sand	2.68	0.52	2.96
Crushed granite sand	2.57	0.80	3.22
River sand	2.59	0.78	2.92

Experimental Procedures of the Wedge Splitting Test

Materials and Mix Proportions of Concrete

River sand and crushed granite sand, as well as crushed limestone sand, were used as fine aggregate for comparison. The physical properties of fine aggregate are given in Table 3. Ordinary Portland cement (ASTM Type I) was used, and the crushed limestone gravel passing the 10-mm sieve was used as coarse aggregate.

Detailed mix proportions of concrete are given in Table 4. A superplastizer SP-20 that meets ASTM C 494 requirements for Type F admixture was used to obtain good workability in low water-binder ratio. Silica fume (SF, Elkem Microsilica) was also used to produce high-strength concrete. The crushed sand concrete was made with water-binder ratios of 20, 40, and 60%, and the river sand concrete was made with water-binder ratios of 20, 30, 40, and 60%.

Specimen Details and Test Method

The size and geometry of the specimen are shown in Figure 3. The initial notch on the specimen was made by inserting a plate inside the specimen during the concrete casting and taking the plate out after 24 h of curing. The groove was made for the stable test by guiding the crack propagation. The specimens were cured in water until 1 h before the test. The loading devices of the WST consist of wedges and rollers, as shown in Figure 4. The wedges are pressed between rollers in order to split the specimen into halves.

During the test, the vertical force (F_v) and crack mouth opening displacement (CMOD)

TABLE 4
Mix Proportions of Concrete

Mix No.*	W/B (%)	Unit weight (kg/m^3)					Admixture (CX%)
		Cement	Water	Sand	Gravel	SF	
L20 G20 R20	20	628	140	522	1059	70	3.5
R30	30	489	154	593	1100	26	2.0
L40 G40 R40	40	423	169	601	1124	–	1.0
L60 G60 R60	60	331	199	726	1002	–	–

L, Crushed limestone sand; G, Crushed granite sand; R, River sand; 20, 30, 40, and 60 designate the water-binder ratio.

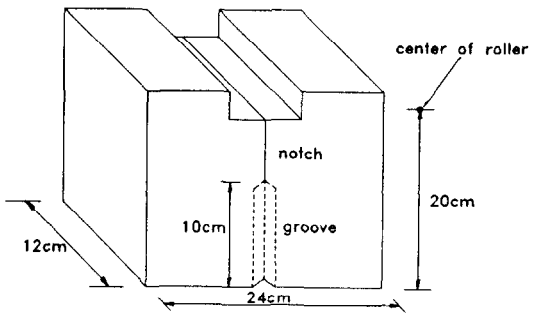

FIG. 3.
Size and geometry of specimen.

were measured, and the horizontal splitting force (F_s) applied on the specimen can be determined as follows.

$$F_s = \frac{F_v}{2 \tan \alpha} \tag{1}$$

where α is the wedge angle (6).

The CMOD was measured by means of a clip gauge. The clip gauge was fixed at the level where the splitting force acted on the specimen, i.e., at the level of the axles of the rollers. In a closed-loop servo-hydraulic testing machine, the test was controlled by CMOD. The test was carried out at a loading rate of 0.002 mm/s, so that the time from the beginning of the test up to the peak load was between 40 and 60 s.

Prior to the WST, the compressive strength of concrete was tested according to ASTM C

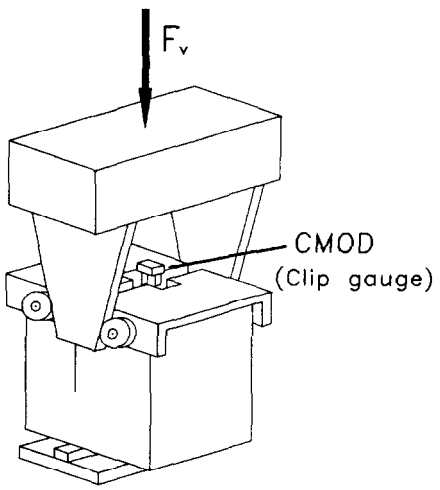

FIG. 4.
Set-up of wedge splitting test.

39, the splitting tensile strength according to ASTM C 496, and the modulus of elasticity according to ASTM C 469, respectively.

Results and Discussion

Test Results

The G_f of concrete by the WST can be obtained directly from the measured load-CMOD curves, i.e., the total area under load-CMOD curve divided by the total ligament area of the specimen (7). Typical load-CMOD curves obtained by the WST method are given in Figure 5. In the load-CMOD curves of Figure 5, load is the F_s. A summary of the test results is given in Table 5, where $F_{s,max}$ is the maximum horizontal splitting force.

Fracture Energy and Characteristic Length

Figure 6 shows the relationship between the G_f and the compressive strength of concrete. As shown in Figure 6, the G_f did not increase proportionally with an increase in compressive strength of concrete. The G_f of concrete increased when the compressive strength of concrete was in the range of 20–60 MPa. The G_f, however, tended to decrease more and less in compressive strengths greater than 60 MPa.

The qualities of concrete are influenced by the content of VFS. As the content of VFS is increased, the unit water content and drying shrinkage of concrete increase, and the setting of concrete accelerates (3). Accordingly, ASTM, JIS, and KS standards have restricted the content of VFS of which the limits in ASTM C 33, JIS A 5004, and KS F 2558 are 7%. However, it has been reported that some VFS improves the cohesion between cement paste and aggregate (1). Due to this improvement in cohesion, it seems that the G_f of crushed sand concrete is slightly higher than that of river sand concrete. However, the G_f of concrete is little influenced by the type of fine aggregate.

In CEB-FIP model code, G_f is defined as functions of the compressive strength of concrete and maximum aggregate size, as follows (10):

$$G_f = G_{fo}\left(\frac{f_{cm}}{f_{cmo}}\right)^{0.7} \tag{2}$$

where $f_{cmo} = 10$ MPa, f_{cm} is the compressive strength of concrete (MPa), and G_{fo} is the base value of fracture energy, which depends on the maximum aggregate size (d_{max}). It was shown that Eq. 2 took the compressive strength of concrete strongly into account, as shown in Figure 6. Thus the following equation was obtained through a regression analysis for a best fitting of test results.

$$G_f = 1041(1 - e^{-0.07f_c'}) \tag{3}$$

The characteristic length (l_{ch}) is an index representing the brittleness of concrete, and is defined as a function of G_f, tensile strength (f_t), and elastic modulus (E_c) (8).

$$l_{ch} = \frac{E_c G_f}{f_t^2} \tag{4}$$

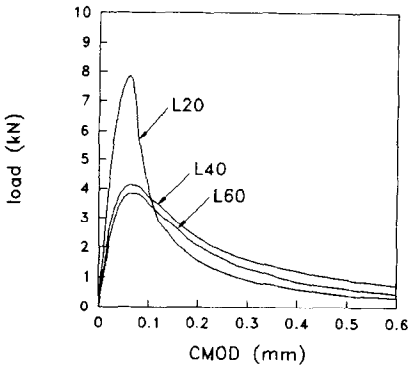

(a) Crushed limestone sand concrete

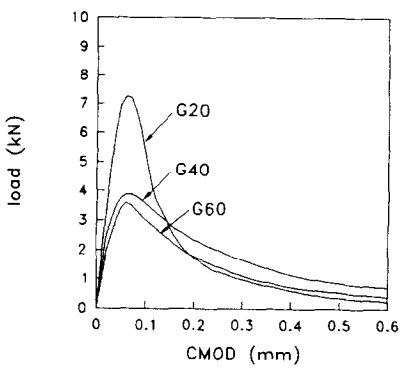

(b) Crushed granite sand concrete

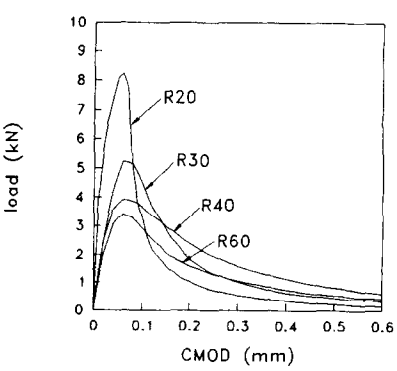

(c) River sand concrete

FIG. 5.

Load-CMOD curves: (*a*) crushed limestone sand concrete; (*b*) crushed granite sand concrete; (*c*) river sand concrete.

TABLE 5
Summary of Test Results

Specimen	f_c' (MPa)	f_{sp} (MPa)	E_c (GPa)	$F_{s,max}$ (kN)	G_f (N/m)	G_f' (N/m)	G_f'/G_f (%)	l_{dn} (mm)
L60	31.27	3.48	29.94	3.85	100.15	11.64	11.63	247.6
L40	47.41	4.61	33.72	4.14	120.45	20.27	16.83	191.1
L20	82.80	6.05	40.57	7.84	104.09	24.68	23.71	115.4
G60	32.57	3.24	28.79	3.64	88.29	10.71	12.13	242.1
G40	45.85	4.78	33.40	3.87	116.14	17.63	15.18	169.8
G20	85.68	6.60	39.57	7.40	113.06	26.60	23.52	102.7
R60	34.87	3.31	26.51	3.39	83.32	11.32	13.59	201.6
R40	55.28	4.69	31.58	3.91	116.36	18.81	16.16	167.1
R30	66.91	5.18	34.35	5.23	98.74	17.52	17.74	126.4
R20	88.80	6.12	38.14	8.24	92.34	24.56	26.60	94.0

The length of the fracture process zone at crack growth is approximately proportional to characteristic length, which is a pure material property (8). The characteristic length calculated by Eq. 4 is given in Figure 7, where the splitting tensile strength of concrete was used instead of the direct tensile strength of concrete.

For the same concrete strength, the characteristic length was not much affected by the type of fine aggregate. As shown in Table 5, the characteristic length of crushed limestone sand concrete was almost the same as that of river sand concrete or crushed granite sand concrete. In addition, characteristic length was strongly dependent on the compressive strength of concrete, as shown in Figure 7. The following equation was obtained through a regression analysis with the test results.

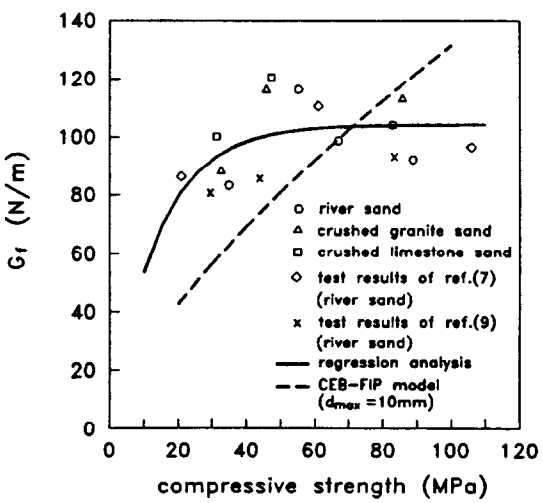

FIG. 6.
Variation of fracture energy with compressive strength of concrete.

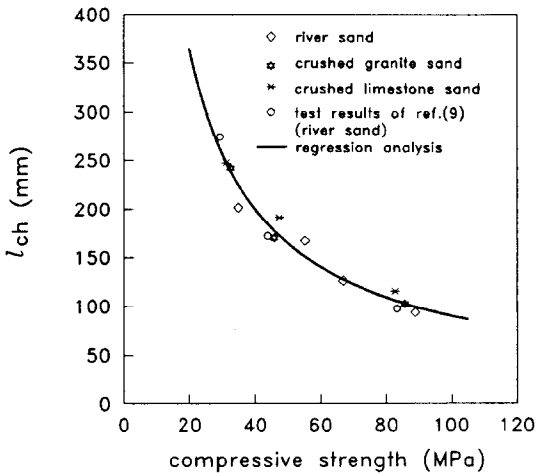

FIG. 7.
Variation of characteristic length with compressive strength of concrete.

$$l_{ch} = 4.94(f_c')^{-0.87} \tag{5}$$

where l_{ch} is the characteristic length in m, and f_c' is the compressive strength of concrete in MPa.

Figure 8 shows the ratio of the pre-peak energy (G_f') to fracture energy (G_f). The pre-peak energy (G_f') is shown in Figure 8. For the same aggregate size, the ratio of G_f'/G_f was increased with the compressive strength of concrete, and was not affected by the type of fine aggregate. Based on regression analysis, G_f'/G_f can be represented as the following equation:

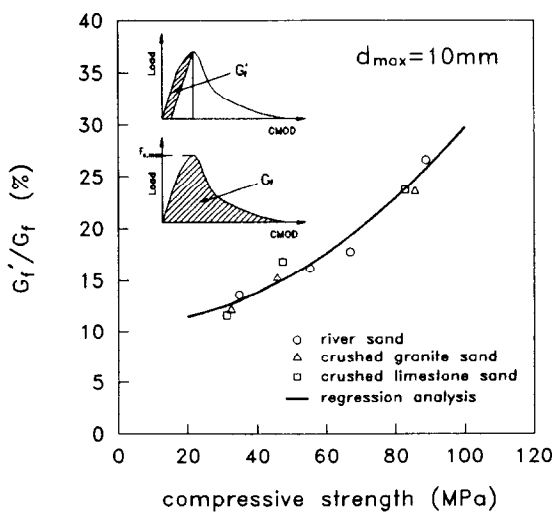

FIG. 8.
Variation of G_f'/G_f with compressive strength of concrete.

$$\frac{G_f'}{G_f} = 10.76 + 0.19 \times 10^{-2} f_c'^{2.0} \quad (8)$$

Although G_f' and G_f are defined as a function of f_c' in this research, the ratio of G_f'/G_f could be influenced by many parameters, i.e., maximum aggregate size, and type of aggregate, as well as the compressive strength of concrete. Therefore, further tests are needed to introduce a more general relation between G_f' and G_f.

Conclusions

From the results of the investigation on the fracture characteristics of crushed limestone sand concrete, the following conclusions can be drawn:

1) The G_f of the crushed sand concrete was slightly higher than that of the river sand concrete. This seems to be due to VFS included in crushed sand, which tends to improve the cohesion between cement paste and aggregate.
2) The characteristic length of crushed limestone sand concrete was almost the same as that of the river sand concrete or the crushed granite sand concrete. Also, the characteristic length greatly decreased as the strength of concrete increased.
3) The G_f was not proportionally increased with increasing the strength of concrete. In addition, the G_f of concrete was little influenced by the type of fine aggregate.
4) For the same aggregate size, the ratio of G_f'/G_f was increased as the compressive strength of concrete was increased, and was not affected by the type of fine aggregate.

Acknowledgment

The authors are grateful to Ministry of Construction and Transportation (MCT) and Samsung Corporation (Engineering & Construction Group) for providing the financial support for the project.

References

1. Committee on Concrete JCA, Cem. Concr. , 36–44 (1993).
2. A. Kronlof, Mater. Struct. 27, 15–25 (1994).
3. V.M. Malhotra and G.G. Carette, ACI J. 82, 363–371 (1985).
4. RILEM Technical Committee 50, Mater. Struct. 18, 285–290 (1985).
5. RILEM Technical Committees 78-MCA and 51-ALC, E&FN SPON, 333–339 (1993).
6. E. Bruhwiler and F.H. Wittmann, Engng. Fract. Mech. 35, 117–125 (1990).
7. J.K. Kim, H. Mihashi, K. Kirikoshi, and T. Narita, Fracture Energy of Concrete with Different Specimen Size and Strength by Wedge Splitting Test. Fracture Mechanics of Concrete Structures, Z.P. Bazant (ed.), pp. 561–566, Elsevier, Amsterdam, 1992.
8. A. Hillerborg, Analysis of One Single Crack Fracture Mechanics of Concrete. Fracture Mechanics of Concrete, F.H. Wittmann (ed.), pp. 223–249, Elsevier, Amsterdam, 1983.
9. J.K. Kim and C.S. Lee, J. Korea Concr. Inst. 7, 129–136 (1995).
10. Comite Euro-International du Beton, CEB-FIP Model Code 1990, Thomas Telford, 1993.